JOURNAL OF MAGNETIC RESONANCE 51, 400–408 (1983)

Chemical Shift Anisotropy in Powdered Solids Studied by 2D FT CP/MAS NMR

AD BAX, NIKOLAUS M. SZEVERENYI, AND GARY E. MACIEL*

Department of Chemistry, Colorado State University, Fort Collins, Colorado 80523

Received June 29, 1982; revised September 28, 1982

A set of new experiments for obtaining the conventional anisotropy powder patterns utilizes a series of π or 2π pulses synchronized with the rotation of the magic-angle spinner. The experiment is most conveniently performed in a two-dimensional fashion. The new pulse sequences are rather insensitive to imperfections of the pulses. Experimental results are shown for hexamethylbenzene and paradimethoxybenzene.

INTRODUCTION

One of the advantages of studying organic molecules in the solid state rather than in the liquid state is the information about the chemical shift anisotropy that can be obtained. Unfortunately a straightforward recording of a ^{13}C spectrum of a nonspinning sample to get the anisotropy information fails in many cases because of the usually extensive overlap of the signals originating from different sites in the molecule, and because of poor sensitivity, due to the fast decay of the signal.

Several types of experiments have been proposed to overcome these problems, at least partially. If sample spinning at the magic angle is used on a compound with a chemical shift anisotropy of the order of the spinning frequency or larger, then spinning sidebands occur in the spectrum which allow the reconstruction of the original anisotropy pattern (*1*, *2*). Dixon (*3*, *4*) recently proposed an experiment for the removal of overlap between the different sidebands and isotropic peaks, making this approach more practical. However, it should be noted that the reconstruction of the anisotropy powder pattern from spinning sidebands is not straightforward. Stejskal *et al.* (*5*) proposed spinning the sample at high speed, but slightly away from the magic angle, giving a line much narrower than in the nonspinning case, but showing the same kind of pattern. Aue *et al.* (*6*) proposed using the spinning sideband reconstruction method via a two-dimensional experiment, giving in some respects the same advantages and disadvantages as the more recent one-dimensional approach of Dixon (*4*). Lippmaa *et al.* (*7*) were the first to propose the application of a series of π pulses that are synchronized with the high-speed magic-angle spinner rotation. The lineshape obtained in this kind of experiment allows the reconstruction of the conventional powder anisotropy pattern. A more elaborate approach has recently been proposed by Yarim-Agaev *et al.* (*8*). They show that a sequence with six π pulses applied during each spinner revolution gives, analogous to Lippmaa's experiment, the opportunity to reconstruct the powder anisotropy pattern, but in a more reliable way. Both the Lippmaa and the Yarim-Agaev experiments are, as the authors point

* To whom correspondence should be addressed.

0022-2364/83/030400-09$03.00/0

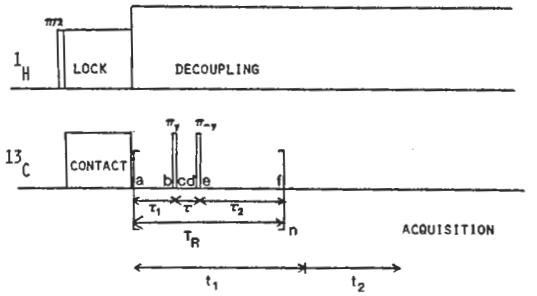

FIG. 1. Schematic representation of the 2π pulse sequence; T_R indicates the rotor period; the evolution period t_1 consists of an integer number n of rotor periods. The initial contact is a standard cross-polarization for enhancing the ^{13}C magnetization.

out, extremely sensitive to pulse imperfections, and also require a two-dimensional approach in the case of nearby resonances.

The experimental approach reported here utilizes two-dimensional Fourier transformation and gives the conventional isotropic spectrum in the F_2 dimension and the corresponding anisotropy patterns in the F_1 dimension. These new experiments are rather insensitive to imperfections of the rf pulses.

EXPERIMENTAL

The hexamethylbenzene and paradimethoxybenzene were obtained from Aldrich Chemical Company and were used as received. The ^{13}C NMR experiments were carried out at 25.27 MHz on a homebuilt spectrometer, using a Nalorac widebore superconducting magnet, a Nicolet 1180 data system, and a Nicolet 293A pulse programmer. The width for a ^{13}C π pulse was 10.9 μsec and for a 2π pulse, 21.0 μsec. A bullet type Kel-F rotor was employed and the spinning speed was adjusted to be 2400 Hz.

RESULTS AND DISCUSSION

The Basic Sequence

In the description of the new sequences it is assumed that the spinning speed is large compared with the width of the anisotropy pattern. In practice this means that spinning sidebands should have a total integrated intensity that is less than about 10 percent of that of the isotropic peak. The pulse sequence for the basic experiment is set out in Fig. 1 and is rather similar to the 2π sequence proposed by Yarim-Agaev *et al.* (*8*). The main differences are the opposite phases of the two π pulses and the fact that our experiment is performed in a two-dimensional fashion. In addition, the time τ between the two π pulses will always be short compared with the time (T_R) needed for a full revolution of the spinner. This latter restriction simplifies the results considerably, as shown below.

The resonance frequency of a nucleus in the kth arbitrary crystallite can always be written as

$$\Omega_K(t) = \Omega_I + \Omega_A(t) \qquad [1a]$$

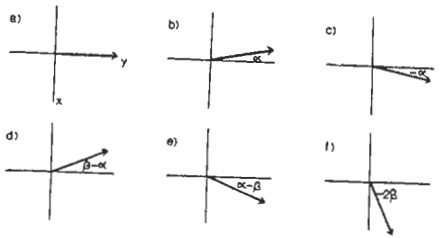

FIG. 2. Evolution of the transverse magnetization of a ^{13}C nucleus in a certain crystallite during the first rotor period. (a)–(f) correspond to the times indicated in Fig. 1.

with

$$\Omega_A(t) = C_1 \cos(\Omega_R t + \phi_1) + C_2 \cos(2\Omega_R t + \phi_2), \qquad [1b]$$

where t is the time starting from the end of cross-polarization, Ω_I is the isotropic shift frequency, Ω_A is the anisotropic contribution, Ω_R is the spinner rotation frequency, and C_1, C_2, ϕ_1, and ϕ_2 are constants that depend on the orientation of the crystallite with respect to the static magnetic field at $t = 0$ (point a in Fig. 1).

In Fig. 2 the evolution of the ^{13}C magnetization vector in the transverse plane from the nucleus in the kth crystallite is shown for different times in the sequence of Fig. 1 during the first revolution of the spinner. Suppose for convenience that $\Omega_I = 0$; i.e., the isotropic ^{13}C shift is on resonance. After cross-polarization the ^{13}C magnetization vector will start out along the y axis (Fig. 2a). Then during a time, τ_1 it covers an angle (α) given by

$$\alpha = \int_0^{\tau_1} \Omega_A(t)dt. \qquad [2]$$

The first π_y pulse rotates the magnetization vector and thereby inverts this angle (Figs. 2b, c). During the time τ between the two π pulses the vector evolves through an angle, β, given by

$$\beta = \int_{\tau_1}^{\tau_1+\tau} \Omega_A(t)dt \qquad [3a]$$

or, if $\tau \ll T_R$,

$$\beta \approx \tau\Omega_A(\tau_1 + \tau/2). \qquad [3b]$$

At the end of the τ period the angle of the vector with respect to the y axis in the rotating frame equals $\beta - \alpha$. The second pulse, a π_{-y} pulse, inverts this angle to $\alpha - \beta$ (Fig. 2e), and during the following interval τ_2, the vector will evolve through an angle, γ, given by

$$\gamma = \int_{\tau_1+\tau}^{T_R} \Omega_A(t)dt. \qquad [4]$$

The total angle evolved through during one revolution of the spinner is given by $\alpha - \beta + \gamma$. Furthermore, it follows from Eq. [1] that

$$\int_0^{T_R} \Omega_A(t)dt = 0 = \alpha + \beta + \gamma. \qquad [5]$$

Hence at the end of the first spinner rotation the vector makes an angle, $\alpha - \beta + \gamma$

$= -2\beta$, with the positive y axis. After n rotations of the spinner the vector will make an angle, $-2n\beta$, with the positive y axis. Therefore, if data acquisition is started after n revolutions of the spinner, for which $t_1 = nT_R$, and a set of experiments is performed with different values of n, then phase modulation of the detected y component of ^{13}C magnetization occurs as a function of t_1. This phase modulation occurs with a frequency, $-2\beta/T_R$, and a two-dimensional Fourier transformation will give a resonance line at

$$(\omega_1, \omega_2) = (-2\beta/T_R, 0) = (-2\tau\Omega_A(\tau_1 + \tau/2)/T_R, 0). \qquad [6]$$

Of course, in the case of a polycrystalline or powdered sample, all possible values for $\Omega_A(\tau_1 + \tau/2)$ occur, corresponding to the different orientations of the crystallites after the end of the cross-polarization at a. Hence, in the F_1 dimension of the 2D spectrum the static powder anisotropy pattern will appear, scaled by a factor $-2\tau/T_R$. In the case of an arbitrary value, Ω_I, for the isotropic chemical shift, the total accumulated phase angle at the beginning of data acquisition will be

$$\alpha - \beta + \gamma + \Omega_I(\tau_1 + \tau_2 - \tau) = -2\beta + \Omega_I(T_R - 2\tau)$$

and the two-dimensional Fourier transformation will give a resonance line at

$$(\omega_1, \omega_2) = (-2\beta/T_R + (T_R - 2\tau)\Omega_I/T_R, \Omega_I). \qquad [7]$$

The Ω_I contribution in the F_1 dimension can easily be removed by the application of a linearly frequency-dependent phase correction, Φ_I, to each of the spectra obtained for a different number (n) of spinner revolutions prior to acquisition, where Φ_I is given by

$$\Phi_I = -2\pi(T_R - 2\tau)n \qquad \text{rad/Hz}. \qquad [8]$$

As phase modulation occurs in this experiment, lines in the two-dimensional spectrum will show a phase-twisted lineshape (*9*, *10*), and no full two-dimensional absorption spectrum can be obtained unless another experiment that generates a so-called reversed-precession signal (*11*) is performed. However, for our purposes this is not necessary because each of the cross sections that cuts the F_2 axis at $\Omega_2 = \Omega_I$, showing the anisotropy pattern, can be phased to the pure absorption mode (*10*).

If the condition, $\tau \ll T_R$, is met, the two ^{13}C π pulses of opposite phase will partially cancel each other's imperfections that are due to such factors as rf inhomogeneity or simply a miscalibration of the π-pulse width. However, the effect of imperfection due to frequency offset of the carbon rf field is not compensated by the phase inversion of the second pulse. Furthermore, the longer the period τ, the less pulse imperfections will be compensated, and adjustment of the length of the π pulses becomes more critical. In practice, a τ value as large as $T_R/10$ causes serious problems.

Compensated Multiple 2π Sequence

In order to avoid the problems of pulse imperfections indicated above, a pulse sequence with better compensating characteristics is clearly desirable. Such a sequence, which relies on the same principles as the one shown in Fig. 1, is shown in Fig. 3. The π_y–τ–π_{-y} ^{13}C sequence is now replaced by an integer number of $2\pi_y$–$2\pi_{-y}$ pulse pairs. The 2π pulses cause an apparent halt in the precession of all the magnetization vectors during the period, τ. This can easily be understood by using average Hamiltonian theory: In the case of a single pair of $2\pi_y$–$2\pi_{-y}$ pulses the

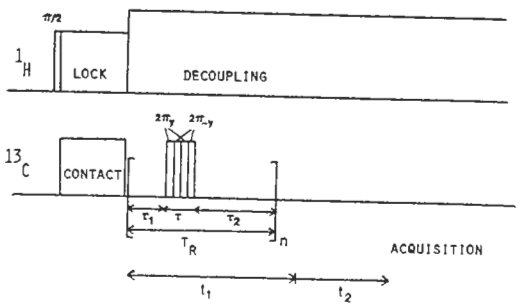

FIG. 3. Schematic representation of the multiple-2π sequence. T_R indicates the rotor period and τ the time during which an integer number of $2\pi_y$–$2\pi_{-y}$ pulse pairs are applied.

Hamiltonian in the rotating frame during the first half of the τ period is given by $+\gamma H_1 I_y$ and during the second half by $-\gamma H_1 I_y$, neglecting the effect of chemical shift. Therefore the average Hamiltonian during the τ period is zero, and no average precession takes place in the rotating frame. Hence, after a complete revolution, the total accumulated phase angle is $\alpha + \gamma = -\beta$, where α, β, and γ are as defined before. Then, using the same arguments as in the previous section, phase modulation of the detected ^{13}C magnetization component will occur with frequency $-\beta/T_R$, where β is again given by Eq. [3]. The interval τ is now the time during which the two 2π pulses are applied. Note that the modulation frequency is halved compared with the experiment described in the previous section. However, this decreased modulation frequency is more than offset by the high degree of compensation of pulse imperfections, causing a slower decay of the signal as a function of t_1, i.e., a higher resolution of the anisotropy powder pattern. Not only pulse imperfections due to rf inhomogeneity or a pulse miscalibration, but also radiofrequency offset imperfections are to a large extent corrected for in the present case. The linear frequency-dependent phase correction Φ_1, which is necessary to remove the isotropic shift contribution in the F_1 dimension, is given by an equation analogous to Eq. [8]:

$$\Phi_1 = -2\pi(T_R - \tau)n \qquad \text{rad/Hz.} \qquad [9]$$

Figure 4 compares the static ^{13}C powder patterns of hexamethylbenzene obtained from (a) a conventional cross-polarization experiment on a nonspinning sample and (b) an experiment using the scheme of Fig. 1, taking a cross section through the 2D spectrum parallel to the F_1 axis at the F_2 frequency of the aromatic carbon. In obtaining the spectrum the number of different t_1 values used was 34, the maximum number allowed by the pulse programmer. Four scans were time-averaged for each value of t_1, giving a total measuring time of approximately 3.5 minutes. The spectrum of Fig. 4a is the result of 5000 accumulations, taking approximately 1.6 hr, and some Gaussian weighting was used to improve the signal-to-noise ratio. No digital filtering was used in the F_1 dimension to obtain the spectrum in Fig. 4b. Experimentally it was found that best results were obtained if proton decoupling was continued during the ^{13}C pulses, but at a sufficiently high-power level to prevent a Hartmann–Hahn contact during the application of the ^{13}C pulses. It is important that an FID for

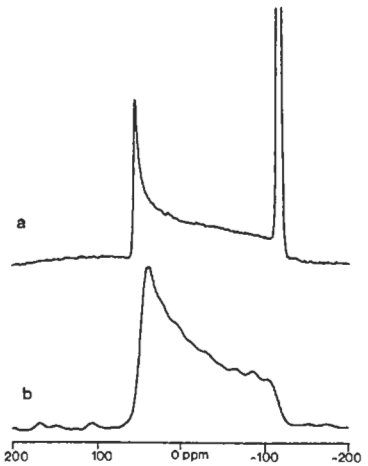

FIG. 4. ^{13}C chemical shift anisotropy patterns for the aromatic carbons in hexamethylbenzene obtained by (a) a conventional cross-polarization experiment on a nonspinning sample and (b) by taking a cross section through the two-dimensional spectrum at the F_2 frequency of the aromatic carbons. The isotropic shift of the aromatic carbons corresponds to 0 ppm. The sequence of Fig. 1 was employed, using 34 different t_1 values and a τ period of 39 μsec. The length of the π pulses was 10.9 μsec.

$t_1 = 0$ and $t_1 = T_R$ (i.e., $n = 0$ and $n = 1$) is obtained, because, if these points are absent in the t_1 domain, significant distortion of the anisotropy pattern can result. In our case these two FIDs could not be obtained automatically, but had to be obtained from separate experiments. In order to calculate the spectral width in the F_1 dimension, the width of the ^{13}C π pulses has to be taken into account. The values for the different delays used were $\tau_1 = 10$ μsec, $\tau = 39$ μsec, and $\tau_2 = 345$ μsec. In practice half the width of a π pulse is added to the τ value, giving a corrected value of 50 μsec. The spectral limits in the F_1 dimension are $\pm(2T_R)^{-1}$, yielding a spectral width of $2(2T_R)^{-1}$. The chemical shift anisotropy was scaled by a factor, $-2\tau/T_R$; hence, the corrected spectral range is given by $\pm(4\tau)^{-1} = \pm 5$ kHz. In order to eliminate the minus sign in the scaling factor, which makes the anisotropy pattern appear to be reversed, the spectrum was reversed in order to give the conventional presentation.

The agreement between the two anisotropy patterns shown in Fig. 4 is fairly good, although the resolution in spectrum (b) appears to be worse than that of spectrum (a). This is due to pulse imperfections, and the fact that τ is not infinitely short, so that no instantaneous frequency is measured, but the average frequency during interval, τ. This averaging effect is clearly visible in the computer-simulated anisotropy patterns shown in the Appendix. Nevertheless, the values for the tensor components, $\sigma_\perp$ and $\sigma_\parallel$, for this axially symmetric molecule can easily be extracted.

Figure 5 shows the anisotropy patterns measured for the four different sites in *p*-dimethoxybenzene, a compound of which the anisotropies had been studied by Maricq and Waugh (*1*) by using the spinning-sideband reconstruction technique. The spectra shown were obtained by using the experiment of Fig. 3, utilizing four 2π

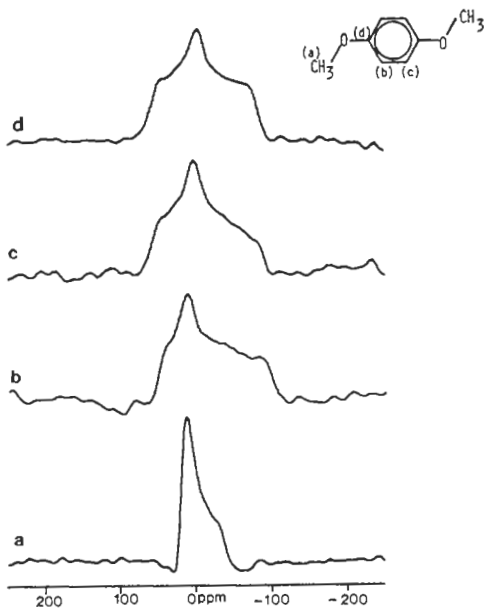

FIG. 5. ^{13}C chemical shift anisotropy patterns for the four different sites in *p*-dimethoxybenzene obtained from cross sections parallel to the F_1 axis through the 2D spectrum at the corresponding shift in the F_2 domain. The sequence of Fig. 3 was employed, using 34 different t_1 values, four 2π pulses of 21 μsec each per τ period and 8 accumulations per t_1 value. The isotropic shift frequencies correspond to 0 ppm.

pulses of 21 μsec each and eight accumulations for each value of t_1. In order to show the "breakpoints" in the powder pattern more clearly, a Lorentzian-to-Gaussian resolution-enhancement filter was applied in the F_1 dimension. The corrected spectral limits in the F_1 dimension are given by $\pm(2\tau)^{-1} = \pm 5.95$ kHz $= \pm 235$ ppm. Using this frequency scale, the values found for σ_{xx}, σ_{yy}, and σ_{zz} in the principal axis system are given in the "measured" column of Table 1. Comparing these values with those obtained by Maricq and Waugh (*1*) shows that all our values are about 25% smaller. This is in full agreement with the results of computer simulations shown in the Appendix, which show that the apparent narrowing of the anisotropy pattern is about 25% for $\tau/T_R = 0.25$. Nevertheless, the overall shape of the anisotropy patterns remains unchanged and the values for σ_{xx}, σ_{yy}, and σ_{zz} can be adjusted for this systematic error, giving the values found in the "adjusted" column of Table 1. The adjusted results are in fair agreement with those obtained by Maricq and Waugh (*1*).

In summary it can be said that the new experiments presented in this paper are convenient ways to obtain the shape of the anisotropy pattern. Especially the multiple 2π sequence is insensitive to adjusting the width of the 2π pulse and is therefore a good choice for routine use; however, it was found that proper tuning of the probe is important in both experiments proposed, in order to minimize phase transients

TABLE 1

MEASURED AND ADJUSTED ^{13}C CHEMICAL SHIFT TENSOR VALUES IN DIMETHOXYBENZENE

Site	Principal tensor component	Measured	Adjusted	Maricq and Waugh (Ref. (*1*))
a(CH_3)	σ_{11}	67	71	80
	σ_{22}	67	71	71
	σ_{33}	28	19	16
b	σ_{11}	166	184	193
	σ_{22}	136	144	134
	σ_{33}	42	18	12
c	σ_{11}	177	196	198
	σ_{22}	130	134	136
	σ_{33}	39	13	23
d	σ_{11}	209	227	230
	σ_{22}	160	162	162
	σ_{33}	95	75	74

Note. All values are referred to TMS = 0 PPM.

during the rise and fall times of the rf pulses. Sensitivity of the new methods is rather good; in our experiments we found it to be a factor of about 5 to 10 less in terms of signal-to-noise ratio, compared with a conventional CP/MAS spectrum obtained in the same measuring time.

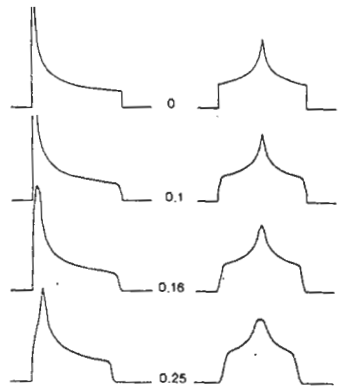

FIG. 6. Computer simulations of anisotropy powder patterns as measured with the sequences of Figs. 1 and 3 for values of τ/T_R varying from 0 to 0.25 from top to bottom. The left half shows the patterns for an axially symmetric chemical shift tensor. The right half is computed with $\sigma_{22} = (\sigma_{11} + \sigma_{33})/2$.

APPENDIX: THE EFFECT OF FINITE τ VALUE ON THE POWDER PATTERN

The orientation of the principal axis system (PAS) in an arbitrarily oriented crystallite is defined by the angles α, β, and γ. Angle α is defined as the angle between the direction of the σ_{33} component of the PAS and the magic-angle axis, which we define to be in the yz plane of our laboratory frame. Angle β is the angle over which the σ_{33} component has to be rotated about the magic-angle axis, in order to fall in the yz plane, and to be in the same half-plane as the positive z axis. Angle γ is defined as the angle through which the PAS has to be rotated about the σ_{33} component (when rotated about β into the zy plane) to bring the σ_{11} component colinear with the positive x axis.

Using these definitions for α, β, and γ, the shift, δ, of the nucleus in this arbitrarily oriented crystallite is given by

$$\delta(\alpha, \beta, \gamma) = (\sqrt{3}^{-1} \cos\alpha + \sqrt{2/3} \cos\beta \sin\alpha)^2\sigma_{33} + (\sqrt{3}^{-1} \sin\alpha \sin\gamma - \sqrt{2/3} \cos\alpha \cos\beta \sin\gamma - \sqrt{2/3} \sin\beta \cos\gamma)^2\sigma_{11} + (\sqrt{3}^{-1} \sin\alpha \cos\gamma - \sqrt{2/3} \cos\alpha \cos\beta \cos\gamma + \sqrt{2/3} \sin\beta \sin\gamma)^2\sigma_{22}.$$

The static powder anisotropy pattern is now simply calculated by integrating δ over the angles α, β, and γ from zero to π. The powder pattern as measured in our experiments is simulated analogously by integrating $\delta(\alpha, \beta, \gamma)$ over β from β_1 to $\beta_1 + 2\pi\tau/T_R$ before integrating over α, β_1, and γ. Figure 6 shows computer simulations for an axially symmetric chemical shift tensor and for one with $\sigma_{22} = (\sigma_{11} + \sigma_{33})/2$. For values $\tau/T_R > 0.25$ the simulated pattern rapidly looses similarity with the static powder pattern as τ/T_R is increased.

No broadening function has been used in the computer simulations. The effect of broadening due to transverse relaxation is to make the broadening contribution due to the finite τ value appear less severe.

ACKNOWLEDGMENTS

The authors are grateful for partial support of this research by grants from the U.S. Geological Survey and the Colorado State University Experiment Station.

REFERENCES

1. M. M. MARICQ AND J. S. WAUGH, *J. Chem. Phys.* **70**, 3300 (1979).
2. J. S. WAUGH, M. M. MARICQ, AND R. CANTOR, *J. Magn. Reson.* **29**, 183 (1978).
3. W. T. DIXON, *J. Magn. Reson.* **44**, 226 (1981).
4. W. T. DIXON, *J. Chem. Phys.* **77**, 1800 (1982).
5. E. O. STEJSKAL, J. SCHAEFER, AND R. A. MCKAY, *J. Magn. Reson.* **25**, 569 (1977).
6. W. P. AUE, D. J. RUBEN, AND R. G. GRIFFIN, *J. Magn. Reson.* **43**, 472 (1981).
7. E. LIPPMAA, M. ALLA, AND T. TUHERM, *in* "Proceedings, 19th Congress Ampère, Heidelberg, 1976," p. 113.
8. Y. YARIM-AGAEV, P. N. TUTUNJIAN, AND J. S. WAUGH, *J. Magn. Reson.* **47**, 51 (1982).
9. G. BODENHAUSEN, R. FREEMAN, R. NIEDERMEYER, AND D. L. TURNER, *J. Magn. Reson.* **26**, 133 (1977).
10. A. BAX, "Two-Dimensional Nuclear Magnetic Resonance in Liquids," pp. 27–31, Reidel, Boston, 1982.
11. P. BACHMANN, W. P. AUE, L. MULLER, AND R. R. ERNST, *J. Magn. Reson.* **28**, 29 (1977).

JOURNAL OF MAGNETIC RESONANCE **51**, 409–423 (1983)

Nuclear Magnetic Relaxation in Multipolar AX Spin Systems. I. The Longitudinal Magnetizations

LAWRENCE G. WERBELOW AND DAVID A. IKENBERRY

Department of Chemistry, New Mexico Institute of Mining and Technology, Socorro, New Mexico 87801

AND

GUY POUZARD

President, Universite de Provence, Place Victor Hugo, 13001 Marseille, Cedex 3, France

Received June 29, 1982

The nuclear magnetic perturbation-response characteristics of the system consisting of a dipolar spin ($I = 1/2$) coupled to a multipolar spin ($I > 1/2$) are considered in detail. It is demonstrated that the natural representation of the time evolution expressions for this system is couched in terms of a nested hierarchy of one-spin, two-spin, . . . , n-spin correlations. It is rationalized that within certain limits, these detailed expressions predict a behavior that differs dramatically from the behavior predicted for either dipole–dipole systems or isolated multipole systems.

INTRODUCTION

Interest in the nuclear magnetic resonance relaxation experiment has increased dramatically in the last few years. This increased interest can be attributed to the realization that various parameters abstracted from the NMR relaxation experiment provide very exacting structural and dynamical information at the molecular level.

Regardless of the wealth of contemporary studies which utilize NMR relaxation techniques, there still exist a number of relatively simple spin groupings where the relaxation behavior has not been examined in detail. This statement is especially pertinent for coupled spin systems containing one or more multipolar ($I > 1/2$) nuclides. Although a number of workers (*1*) have contributed to the understanding of relaxation effects in coupled, multipolar spin systems, it still remains an area of investigation that has received relatively little attention. However, since three-fourths

0022-2364/83/030409-15$03.00/0